Photoelectrons from resonant ionization of Na_2: angular and non-Franck–Condon energy distributions

Robert G. Daniel, James S. Keller, Dina Pines and R. Stephen Berry
The Department of Chemistry and James Franck Institute, Chicago, IL 60637, USA

Received 31 Augustus 1990; in final form 8 May 1991

We present energy and angular distributions of photoelectrons from the resonant two-photon, two-color ionization of sodium dimer through particular rovibronic levels of the B $^1\Pi_u$ and A $^1\Sigma_u^+$ state. The vibrational state distributions of the ion core produced from the B state do not correspond to Franck–Condon distributions, according to the photoelectron energy spectra. Non-Franck–Condon distributions of final states were observed at two ionizing wavelengths, and through all the four intermediate rovibrational levels of the B state studied here. Ionization through the A state showed a Franck–Condon-like distribution of final states. At best, plausible conjectures can be suggested to account for the non-Franck–Condon behavior of the B state.

1. Introduction

In this Letter we report energy and angular distributions of molecular photoelectrons resulting from the resonant photoionization of Na_2 via the B $^1\Pi_u$ and A $^1\Sigma_u^+$ states as intermediates. We expected the photoelectron angular distributions to vary with the rotational state transition (P versus Q versus R branch), the intermediate vibrational state, and possibly the final vibrational state of the ion. Previous work shows dependence of angular distributions upon the final ion vibrational [1] and rotational [2] states, but in light of the results reported here, it seems that a full understanding of the process involved has yet to be reached. Recent theoretical results have demonstrated that non-Franck–Condon effects can arise from the photoionization of molecules having repulsive doubly excited states, shape resonances or Cooper minima [3].

Previous theoretical work [4] made predictions of the form of photoelectron angular distributions expected from resonant two-photon ionization of molecular sodium. Angular distributions are expected to depend on the type of rotational transition to the intermediate state (P, Q, or R branch), the intermediate electronic state, the Hund's coupling case, the final vibrational state, and, as a consequence of selection rules, the rotational level of the corresponding ion. We set out to test this theory and to explore the possible exchange of energy and angular momentum between the ion core and the ejected photoelectron. The following transitions from the ground X state to the excited A and B states were investigated in this study:

to the excited B state,

$$^1\Sigma_g^+(v=0, j=10) \rightarrow {}^1\Pi_u(v=3, j=10), \quad \mathrm{Q}(10),$$

$$^1\Sigma_g^+(v=0, j=18) \rightarrow {}^1\Pi_u(v=3, j=19), \quad \mathrm{R}(18),$$

$$^1\Sigma_g^+(v=0, j=17) \rightarrow {}^1\Pi_u(v=4, j=18), \quad \mathrm{R}(17),$$

$$^1\Sigma_g^+(v=0, j=15) \rightarrow {}^1\Pi_u(v=4, j=14), \quad \mathrm{P}(15);$$

and to the excited A state,

$$^1\Sigma_g^+(v=0, j=5, 9) \rightarrow {}^1\Sigma_u^+(v=4, j=4, 10),$$

$$\mathrm{P}(5)+\mathrm{R}(9).$$

Experiments are presently underway to extend the study of the A $^1\Sigma_u^+$ state as the intermediate.

2. Experimental

Most of the apparatus used for these experiments has been described in detail elsewhere [5], so is outlined here only briefly. The molecular beam is pro-

0009-2614/91/$ 03.50 © 1991 – Elsevier Science Publishers B.V. (North-Holland)

duced by a "pick-up beam" source [6] consisting of an effusive beam of sodium which crosses a pulsed beam of argon within a few millimeters of the 0.8 mm solenoid valve orifice. Sodium picked up by the argon beam is cooled to an estimated 30 K; the sodium/argon molecular beam passes through a 3 mm skimmer approximately 2 cm downstream from the pulsed valve into an interaction chamber pumped to 10^{-6} Torr. The alkali oven has two stages, each capable of being heated to 1000 K. The oven neck is kept 50 to 150°C warmer than the body to prevent the 250 μm orifice from clogging. Although alignment of molecules in molecular beams at high pressure has been reported [7], we observed the same angular distributions of photoelectrons at high and low oven temperatures and believe that the orientation of our target molecules are isotropically distributed.

The sodium/argon beam is crossed at right angles by linearly polarized collinear laser beams. The intersection is at the center of two concentric copper spheres which provide a 3.5 cm field-free drift path and a 1 cm acceleration region for ejected photoelectrons. The drift region is used as a time-of-flight electron energy analyzer; the path is short but adequate for the present experiments, specifically to resolve, at our ionizing energies, photoelectrons corresponding to different final vibrational states of the ion core. The detector is a channeltron electron multiplier on an axis mutually perpendicular to the molecular beam and the collinear laser beams. The detector is fixed; angular distributions are obtained by rotating the polarization vectors of the laser beams. Windows of stainless steel wire mesh of 90% transmittance allow the photoelectrons to pass through the spheres. A copper tube extending through the inner sphere to the outer sphere was inserted to prevent field penetration through the 3/4 inch entrance and exit holes for the laser beams; sections milled out of the tube allow passage of the molecular beam and the photoelectrons. The spheres and copper tube are cleaned with dilute HCl between experimental runs to prevent buildup of any sodium/sodiumoxide/sodiumhydroxide, which can produce background electrons from scattered light. The count rate was kept to less than 1 electron per laser pulse during data collection. The electron energy distributions widened and their flight times increased during the course of a run; these were attributed to build-up of sodium on the spheres.

The laser system consists of two dye lasers pumped by an excimer laser, running with a mixture of xenon and chlorine. The exciting laser is operated with coumarin 481 and has a bandwidth of 0.08 cm^{-1}, which allows an individual rotational line to be excited in the intermediate vibrational state. The beam is passed through a dispersing prism to divert the superradiant component and, thereby, to reduce background counts. This is possible because the exciting wavelengths used were well away from the center of the dye gain curve. The ionizing radiation was produced by a homemade flowing-dye laser, with wavelengths chosen to produce photoelectrons with 100 to 300 meV energy, depending upon the final vibrational state of the ion. Both laser beams were passed through polarizers and double Fresnel rhombs to allow the rotation of the polarization vectors of the beams. Both lasers were focused approximately 20 cm in front of the interaction region with 500 mm focus length lenses to reduce intense fields that contribute background from non-resonant two-photon processes. Electron intensities were checked and found to be linear with respect to both laser beams. The synchronization of the molecular beam and lasers was monitored with a fast ion gauge [8]. The duration of the gas pulse was typically 180–220 μs fwhm.

The B state transitions used for this study, R(18) and Q(10) in the (3, 0) band, and P(15) and R(17) in the (4, 0) band, were chosen because they were well separated from adjacent transitions, and were strong enough to give sufficient count rates during an experiment. The A state transition was chosen to compare with the results of the B state; experiments are presently underway to use isolated R and P branches as intermediates. Contours of the vibrational bands allowed the estimation of the rotational temperature of the molecular beam. The states were identified by first simulating the spectrum using Dunham coefficients [9,10], and then matching the simulated spectrum with one constructed by collecting all electrons when scanning the exciting laser. Two ionizing wavelengths were employed in the first set of experiments. These were chosen by scanning the ionizer to find "quiet" regions in the ionization spectrum of the hot bands of Na_2. The ionizing wavelengths were also chosen to avoid the known

two-photon resonances of the dimer[#1] from $v' = 1, 2$, etc. The two chosen wavelengths were 505 and 499 nm, which correspond to final photoelectron energies of 120 and 150 meV from the ground vibrational state of the ion.

The calibration to convert flight times of the photoelectrons to energies was a crucial part of the analysis. This was carried out by collecting energy distributions of photoelectrons from resonant two-photon, two-color ionization of Na monomer. The monomer was first excited to the $3p\,^2P_{1/2}$ state with rhodamine 590, and then ionized with either a dye laser (using BBQ) or the excimer laser. The electron kinetic energy ranges of 25 to 350 meV and around 1 eV were examined, and the distributions of drift times of the photoelectrons were determined for each. The arrival times computed from naive expectations of times of flight differ significantly from the somewhat longer experimental arrival times; the distributions for "monochromatic" electrons have distinct, apparatus-dependent peak shapes. These are attributed primarily to the finite range within which the electrons are accelerated in the region between the spheres, as well as to small stray fields. The arrival times and fwhm peak widths were plotted versus energy (fig. 1) to produce calibration curves for the photoelectrons. The energies shown in these plots are the nominal final kinetic energies of the electrons, the differences between the ionization potential of sodium and the sum of the laser frequencies.

The distributions of final vibrational states of the parent ions were determined from the final kinetic energies of the photoelectrons inferred from this calibration. An offset delaying the photoelectron arrival time was found to depend on the initializing event of the experiment, normally a pulse generated by a fast photodiode triggered by a small portion of the excimer beam. Despite the day-to-day variation in the offset, calibration curves produced on successive days have nearly identical shapes. This offset was constant across the entire energy range examined. Data from different runs had to be shifted to correct for this day-to-day shift, and calibrations of flight times had to be done for every run. This shift is then used to correct the molecular photoelectron flight

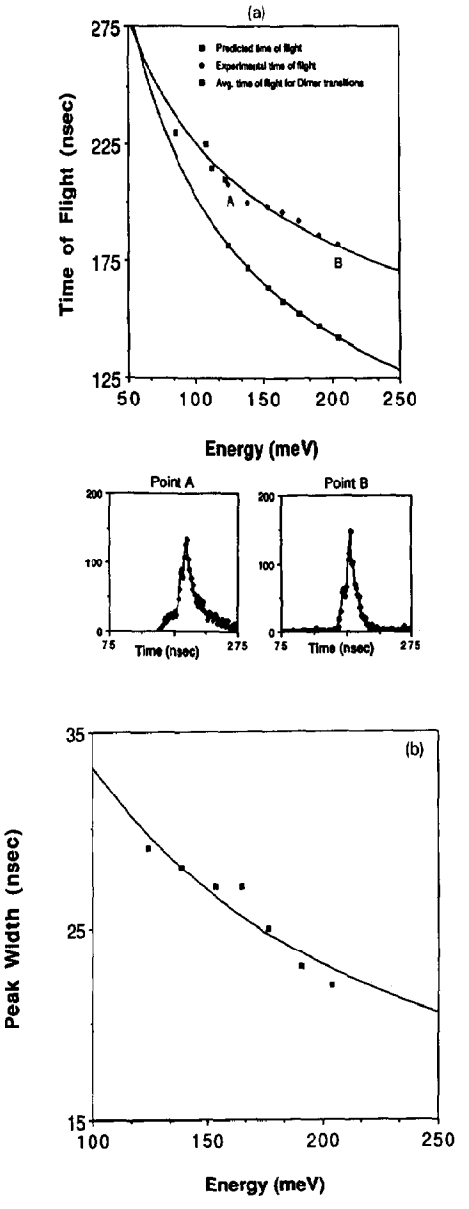

Fig. 1. Plots of the calibration curves used to determine the initial kinetic energy of the molecular photoelectrons. In (a) are the plots of both experimental (top curve) and naively calculated time of flight versus energy. The top curve is used to calculate the initial kinetic energy of the collected photoelectrons. In (b) is the plot of peak width (fwhm) versus energy. This curve is used as a check on the arrival time of the photoelectrons. The small inserts A and B show the shapes of the electron energy distributions of the corresponding points on the energy scale in (a).

[#1] Line positions calculated from potentials of the X, A, and B states in refs. [9,11].

times before calculating the initial kinetic energy of the electron and final vibrational state of the ionic core.

The energy resolution of the apparatus was checked with the monomer energy distributions. The apparatus was found to have constant sensitivity to electrons with any energy in the range examined. We wish to observe electron distributions from ion vibrational states separated by 15 meV. It was determined that when a photoelectron's initial kinetic energy was between 100 and 300 meV, the energy resolution of the apparatus is 10 to 12 meV, sufficient to resolve the ion vibrational states of Na_2^+. This is the energy range of photoelectrons produced in these experiments with either 499 or 505 nm radiation. Ionization from one-color, multiphoton processes was negligible.

3. Results and discussion

Tables 1 and 2 list the least-squares fits of the angular distributions of photoelectrons to the equation

$$I(\theta)=1+C_{20}P_{20}(\cos\theta)+C_{40}P_{40}(\cos\theta)\,,$$

where the $P_{lm}(\cos\theta)$ are associated Legendre polynomials, and the angle θ is the angle between the ionizing laser's polarization vector and the path of the electron to the detector (fig. 2). Distributions were collected for both parallel ($\eta=0°$) and crossed ($\eta=90°$) polarizations. All data were reproduced on successive runs. The fits were also performed with the $C_{60}P_{60}(\cos\theta)$ term included in the expansion. The coefficients C_{60} were found to be zero within experimental error, as expected.

As shown in table 1, a relatively weak energy dependence was found in the angular distributions over the ionizing energies used to probe the B state. The coefficients C_{ij} did not depend on η for the Q branch angular distributions. Both the R and P branch transitions did show different angular distributions for parallel and crossed polarizations ($\eta=0°$ and $90°$).

Table 1
Phenomenological parameters for the $B\,^1\Pi_u$ (3, 0) band transitions

Transition (nm)	η (deg)	C_{lm}
R(18)+499	0	$C_{20}=+1.461\pm0.062$
		$C_{40}=+0.107\pm0.076$
	90	$C_{20}=-0.914\pm0.043$
		$C_{40}=+0.114\pm0.072$
R(18)+505	0	$C_{20}=+0.974\pm0.044$
		$C_{40}=+0.070\pm0.054$
	90	$C_{20}=-0.664\pm0.045$
		$C_{40}=-0.032\pm0.072$
Q(10)+499	0	$C_{20}=+1.011\pm0.068$
		$C_{40}=+0.054\pm0.058$
	90	$C_{20}=+1.364\pm0.037$
		$C_{40}=+0.135\pm0.046$
Q(10)+505	0	$C_{20}=+1.303\pm0.042$
		$C_{40}=+0.035\pm0.049$
	90	$C_{20}=+0.711\pm0.039$
		$C_{40}=+0.038\pm0.048$

Table 2
Phenomenological parameters for the $B\,^1\Pi_u$ (4, 0) band transitions

Transition (nm)	η (deg)	C_{lm}
P(15)+499	0	$C_{20}=+1.214\pm0.099$
		$C_{40}=+0.262\pm0.120$
	90	$C_{20}=-0.655\pm0.062$
		$C_{40}=+0.001\pm0.096$
R(17)+499	0	$C_{20}=+1.464\pm0.081$
		$C_{40}=+0.138\pm0.101$
	90	$C_{20}=-0.837\pm0.075$
		$C_{40}=+0.132\pm0.123$

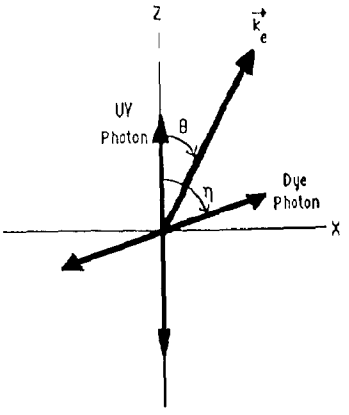

Fig. 2. Schematic of the system geometry. The collinear plane-polarized laser beams, propagating out of the page, intersect the molecular beam at the origin. The polarization vector of the ionizing beam defines the z axis; the angle between the polarization vectors of the ionizing and exciting laser beams is denoted η. The momentum vector $\boldsymbol{k}_e$ of the photoelectron is in the plane of the paper at an angle θ from the z axis.

A surprising result came from the energy distributions from the B state. For each of the transitions studied, the energy distributions from the time-of-flight detection were dominated by a single vibrational state of the molecular ion core. This was the case for both ionizing wavelengths, as well as for all angles η. Only the $v=2$ state of the ion core was unambiguously observed from the (3, 0) band and likewise the $v=3$ state from the (4, 0) band. These, both from $\Delta v=-1$, are the most probable final states of the Franck–Condon envelope. This strong dominance was not expected because the Franck–Condon factors for the $B\,^1\Pi_u \rightarrow X\,^2\Sigma_g^+$ transition are not sharply peaked (table 3 (A)): we expected to observe more than one state of the ion core, particularly from the transition $\Delta v=-2$. Based on the po-

Table 3

(A) Calculated Franck–Condon factors for the $B\,^1\Pi_u \rightarrow X\,^2\Sigma_g^+$ transition using the potentials of Kusch and Henriet [9,12]. (B) Franck–Condon factors for the $B\,^1\Pi_u \rightarrow$highly excited Rydberg state from ref. [13]. (C) Calculated Franck–Condon factors for the $A\,^1\Sigma_u^+ \rightarrow X\,^2\Sigma_g^+$ transition using the potentials of Zemke and Henriet [11,12]

A	v'	v_{ion}								
		0	1	2	3	4	5	6	7	8
	0	0.608	0.283	0.081	0.022	0.005	–	–	–	–
	1	0.323	0.160	0.286	0.147	0.058	0.017	0.004	0.001	–
	2	0.058	0.408	0.016	0.196	0.177	0.092	0.034	0.011	0.003
	3	0.004	0.136	0.379	0.004	0.107	0.167	0.115	0.054	0.021
	4	–	0.013	0.211	0.307	0.038	0.004	0.136	0.125	0.072
	5	–	–	0.027	0.274	0.229	0.078	0.009	0.098	0.123
	6	–	–	–	0.044	0.322	0.161	0.106	0.000	0.062
	7	–	–	–	–	0.063	0.357	0.108	0.119	0.005
	8	–	–	–	–	0.001	0.081	0.383	0.070	0.120
B	v'	v_{Ryd}								
		0	1	2	3	4	5	6	7	8
	0	0.480	0.317	0.135	0.047	0.004	0.001	–	–	–
	1	0.389	0.037	0.216	0.189	0.101	0.043	0.016	0.005	0.002
	2	0.115	0.369	0.013	0.081	0.163	0.131	0.073	0.034	0.014
	3	0.015	0.230	0.240	0.082	0.011	0.103	0.129	0.095	0.053
	4	–	0.044	0.307	0.120	0.132	0.002	0.047	0.105	0.102
	5	–	0.003	0.084	0.343	0.044	0.143	0.024	0.013	0.072
	6	–	–	0.006	0.128	0.347	0.008	0.125	0.053	0.000
	7	–	–	–	0.010	0.172	0.331	0.000	0.095	0.074
	8	–	–	–	–	0.015	0.214	0.307	0.006	0.063
C	v'	v_{ion}								
		0	1	2	3	4	5	6	7	8
	0	0.928	0.069	0.001	–	–	–	–	–	–
	1	0.067	0.803	0.128	0.001	–	–	–	–	–
	2	0.004	0.112	0.701	0.178	0.003	–	–	–	–
	3	–	0.012	0.144	0.616	0.221	0.004	–	–	–
	4	–	0.001	0.021	0.165	0.547	0.257	0.005	–	–
	5	–	–	0.003	0.031	0.178	0.491	0.289	0.006	–
	6	–	–	–	0.004	0.042	0.184	0.445	0.316	0.006
	7	–	–	–	–	0.007	0.050	0.186	0.407	0.341
	8	–	–	–	–	–	0.009	0.059	0.184	0.377

tential curves of Kusch and Hessel [9] and Henriet [12], the intensity ratio for the two most probable Franck–Condon transitions is 2.26:1 in the (3, 0) band; the ratio is 1.45:1 in the (4, 0) band. These ratios imply that at least two vibrational states of Na_2^+ should be populated with sufficient probability to be observed. The calculations have been checked with other proposed potential curves and by two algorithms, and all the results are in close agreement; the process apparently does not follow the Franck–Condon principle. Figs. 3a and 3b show predicted and actual energy contours to illustrate the non-Franck–Condon profile observed. The high kinetic energy ranges are particularly depleted.

To construct predicted contours, we scaled the areas of the energy distributions of monomer photoelectrons by the calculated Franck–Condon factors, and positioned the peak of each distribution to correspond to the calibrated time of arrival for that vibrational ion core, and then summed the total intensities. Weak $\Delta v=0$ and $+1$ transitions may well contribute to the slow electron tails; these, expected to contribute less than 5% to the total intensity, were included in the predicted curves. Consequently, our data imply that only one vibrational ion core strongly dominates each profile, and there is no clear evi-

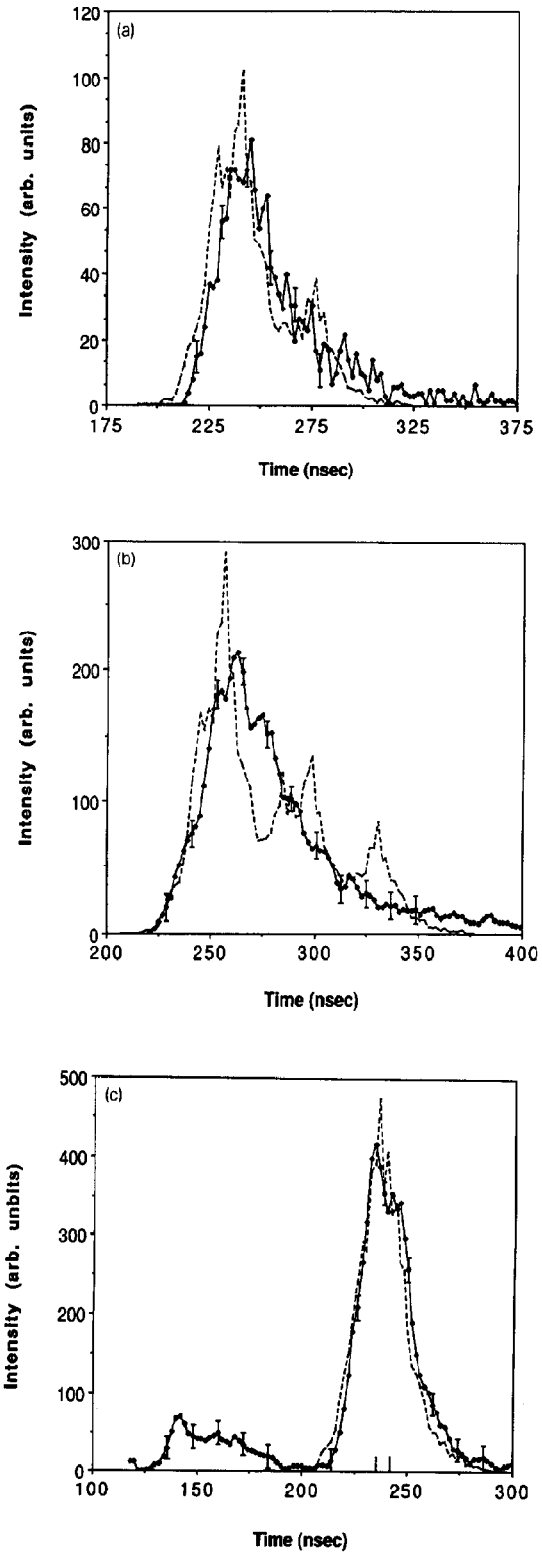

Fig. 3. Sample energy distributions of actual data and the predicted Franck–Condon distributions including the two most probable vibrational states of the ion. Shown in (a) is the R(17) transition of the B state, then ionized with 499.4 nm light, $\eta=0°$, which has a fwhm of 32 ns. In (b) is the Q (10) transition of the B state, then ionized with 505.0 nm light, $\eta=90°$, showing the peak broadening which occurs from sodium buildup on the spheres. In (c) are the overlapping P(5)+R(9) transitions of the A state ionized with 386.3 nm light, with $\eta=90°$ showing the two peaks visible from more than one ion vibrational core being present. The solid curve represents the collected data: the dashed curve is a simulated Franck–Condon envelope containing all energetically accessable vibrational states, based on line shapes of fig. 1, A through B. In both (a) and (b), our resolution is adequate to rule out the possibility of the second-most-likely final vibrational state according to the Franck–Condon factors. In (a), the two most prominent peaks correspond to photoelectrons of $\approx$95 and 112 meV, in (b) to $\approx$72 and 90 meV, and in (c) to $\approx$78 and 85 meV. The early electrons in (c) are attributed to scattered UV radiation photoionizing sodium monomer present in the beam. The two states predicted to be most prominent are indicated by the tick marks on the x axis, $\Delta v=0$ and $+1$. (–●–) collected energy distribution; (– – –) simulated Franck–Condon envelope.

dence for more than one final vibrational level of Na_2^+ from the Na_2^* B state. The evidence for our conclusion is the differences between the simulated and collected energy distributions. The significance of these differences is shown by a χ^2 test to measure the validity of our assumption of Franck–Condon behavior. The B state gave χ^2 values exceeding 1100, while the A state values were in the 1% assurance range. A vibrationally autoionizing state, particularly a $^1\Delta_g$ resonance of the molecule, might be excited in the ionizing step, and conceivably yield a single final vibrational state according to the $\Delta v = -1$ propensity rule, as an alternative to direct ionization. However, as shown in table 3(B), a Rydberg-like resonance should reflect a Franck–Condon distribution of vibrational levels generated from the B state and, thereby, lead to more than one final vibrational state of the ion core. This transition is unlikely an explanation as the ionization energy would produce a $^1\Delta_g$ state in approximately the 9th vibrational level. This is inconsistent with the observed photoelectron energies. In the previous studies of other molecules, several vibrational ion cores have been observed [1], although situations have been described [3] in which non-Franck–Condon effects occur in diatomics.

The preliminary results from the A state do show a Franck–Condon-like energy profile. The calculated ratio based on the potentials of Zemke et al. [11] and Henriet [12] is 2.12:1 while our experimental ratio is 1.21:1. The evidence for two vibrational states of the ion is strengthened by the fact that the two strong peaks from the A state have different angular distributions (table 4). This makes the B state results all the more puzzling. The angular distributions of the B state photoelectrons remain nearly constant across their energy distributions. An electronic $^1\Delta_g$ resonance or a resonance specific to the lower $v_{ion} = 2$, 3 levels and not appearing for $v_{ion} = 4$ or 5 would rationalize the observations.

However the only suitable, known $^1\Delta_g$ electronic states of Na_2^* in the appropriate energy region are g-Rydberg states built on the $^2\Sigma_g^+$ ion core [14]. To reach the energies of these experiments, the B→Rydberg excitation of the lowest of these Rydberg states would have to excite vibrations $v_{Ryd} \approx 9$. Then precisely five or six vibrational quanta, not just one, would have to be transmitted selectively to the autoionizing electron. This is simply too implausible to be accepted. Likewise, a Rydberg state with just the right energy to lead to $\Delta v = -1$ autoionization would have $n \approx 30$, and would be singled out for excitation among all its neighboring Rydberg levels, as well as display a surprising non-Franck–Condon distribution in its excitation from the B state. Hence we shall have to look further, perhaps to a shape resonance or Cooper minimum, for a rationalization of the non-Franck–Condon behavior.

Further experiments are being performed through another vibrational band of the A state to confirm the results form the (4, 0) band. A later paper will present the microscopic parameters implied by the angular distributions of photoelectrons.

Table 4
Phenomenological parameters for the $A\,^1\Sigma_u^+$ P(5)+R(9) transitions ionized with 386.3 nm light

Transition	η (deg)	C_{lm}
$v_{ion}=4$	0	$C_{20}=+0.366\pm0.098$
		$C_{40}=+0.086\pm0.125$
	90	$C_{20}=+0.534\pm0.103$
		$C_{40}=+0.288\pm0.127$
$v_{ion}=5$	0	$C_{20}=+0.317\pm0.117$
		$C_{40}=+0.311\pm0.152$
	90	$C_{20}=+1.016\pm0.143$
		$C_{40}=-0.130\pm0.181$

Acknowledgement

This work has been supported by a Grant from the National Science Foundation.

References

[1] S.T. Pratt, P.M. Dehmer and J.L. Dehmer, J. Chem. Phys. 85 (1986) 3379.
[2] S.W. Allendorf, D.J. Leahy, D.C. Jacobs and R.N. Zare, J. Chem. Phys. 91 (1989) 2216.
[3] J.A. Stephens and V. McKoy, Phys. Rev. Letters 62 (1989) 889, and refs. [3–9] therein.
[4] J.C. Hansen and R.S. Berry, J. Chem. Phys. 80 (1984) 4078;
R.-L. Chien, J. Chem. Phys. 81 (1984) 4023;
S.N. Dixit, D.L. Lynch, V. McKoy and W.M. Huo, Phys. Rev. A 32 (1985) 1267;
S.N. Dixit and V. McKoy, J. Chem. Phys. 82 (1985) 3546.

[5] J.C. Hansen, J.A. Duncanson Jr., R.-L. Chien and R.S. Berry, Phys. Rev. A 21 (1980) 222;
M.P. Strand, J. Hansen, R.-L. Chien and R.S. Berry, Chem. Phys. Letters 59 (1978) 205;
R.-L. Chien, O.C. Mullins and R.S. Berry, Phys. Rev. A 28 (1983) 2078;
J.S. Keller, doctoral dissertation, The University of Chicago (1989).
[6] C.P. Schulz, R. Haughstätter, H.U. Tittes and I.V. Hertel, Phys. Rev. Letters 57 (1986) 1703.
[7] C.P. Sinha, A. Schultz and R.N. Zare, J. Chem. Phys. 58 (1973) 549.
[8] W.R. Gentry and C.F. Giese, Rev. Sci. Instr. 49 (1978) 595.
[9] P. Kusch and M.M. Hessel, J. Chem. Phys. 68 (1978) 2591.
[10] M.E. Kaminsky, J. Chem. Phys. 66 (1977) 495.
[11] W.T. Zemke, K.K. Verma, T. Vu and W.C. Stwalley, J. Mol. Spectry. 85 (1981) 150.
[12] A. Henriet, J. Phys. B 18 (1985) 3085.
[13] M.Ch. Bordas, M. Broyer, J. Chevaleyre, P. Labiastie and S. Martin, J. Phys. (Paris) 46 (1985) 27.
[14] N.W. Carlson, A.J. Taylor, K.M. Jones and A.L. Schawlow, Phys. Rev. A 24 (1981) 822;
S. Martin, J. Chevaleyre, S. Valignat, J.P. Perrot, M. Broyer, B. Cabaud and A. Hoareau, Chem. Phys. Letters 87 (1982) 235.